Graphene-assisted control of coupling between optical waveguides

Andrea Locatelli,[1*] Antonio-Daniele Capobianco,[2] Michele Midrio,[3] Stefano Boscolo,[3] and Costantino De Angelis[1]

[1]*Dipartimento di Ingegneria dell'Informazione, Università degli Studi di Brescia, Brescia 25123, Italy.*
[2]*Dipartimento di Ingegneria dell'Informazione, Università degli Studi di Padova, Padova 35131, Italy.*
[3]*Dipartimento di Ingegneria Elettrica Gestionale e Meccanica, Università degli Studi di Udine, Udine 33100, Italy.*
[*]*andrea.locatelli@ing.unibs.it*

Abstract: The unique properties of optical waveguides electrically controlled by means of graphene layers are investigated. We demonstrate that, thanks to tunable losses induced by graphene layers, a careful design of silicon on silica ridge waveguides can be used to explore passive PT-symmetry breaking in directional couplers. We prove that the exceptional point of the system can be probed by varying the applied voltage and we thus propose very compact photonic structures which can be exploited to control coupling between waveguides and to tailor discrete diffraction in arrays.

OCIS codes: (130.2790) Guided waves; (230.2090) Electro-optical devices; (130.4815) Optical switching devices; (250.7360) Waveguide modulators; (050.1940) Diffraction.

References and links

1. K. S. Novoselov, A. K. Geim, S. V. Morozov, D. Jiang, Y. Zhang, S. V. Dubonos, I. V. Grigorieva, and A. A. Firsov, "Electric field effect in atomically thin carbon films," Science **306,** 666–669 (2004).
2. K. Kim, J. Y. Choi, T. Kim, S. H. Cho, and H. J. Chung, "A role for graphene in silicon-based semiconductor devices," Nature (London) **479,** 338–344 (2011).
3. A. Vakil, and N. Engheta, "Transformation optics using graphene," Science **332,** 1291–1294 (2011).
4. F. Bonaccorso, Z. Sun, T. Hasan, and A. C. Ferrari, "Graphene photonics and optoelectronics," Nat. Photon. **4,** 611–622 (2010).
5. M. Liu, X. Yin, E. Ulin-Avila, B. Geng, T. Zentgraf, L. Ju, F. Wang, and X. Zhang, "A graphene-based broadband optical modulator," Nature (London) **474,** 64–67 (2011).
6. M. Liu, X. Yin, and X. Zhang, "Double-layer graphene optical modulator," Nano Lett. **12,** 1482–1485 (2012).
7. M. Midrio, S. Boscolo, M. Moresco, M. Romagnoli, C. De Angelis, A. Locatelli, and A.-D. Capobianco, "Graphene-assisted critically-coupled optical ring modulator," Opt. Express **20,** 23144–23155 (2012).
8. Q. Bao, H. Zhang, B. Wang, Z. Ni, C. Lim, Y. Wang, D. Y. Tang, and K. P. Loh, "Broadband graphene polarizer," Nat. Photon. **5,** 411–415 (2011).
9. J. T. Kim, and C. G. Choi, "Graphene-based polymer waveguide polarizer," Opt. Express **20,** 3556–3562 (2012).
10. Z. Q. Li, E. A. Henriksen, Z. Jiang, Z. Hao, M. C. Martin, P. Kim, H. L. Stormer, and D. N. Basov, "Dirac charge dynamics in graphene by infrared spectroscopy," Nat. Phys. **4,** 532–535 (2008).
11. S. Klaiman, U. Gunther, and N. Moiseyev, "Visualization of branch points in PT-symmetric waveguides," Phys. Rev. Lett. **101,** 080402(1–4) (2008).
12. A. Guo, G. J. Salamo, D. Duchesne, R. Morandotti, M. Volatier-Ravat, V. Aimez, G. A. Siviloglou, and D. N. Christodoulides, "Observation of PT-symmetry breaking in complex optical potentials," Phys. Rev. Lett. **103,** 093902(1–4) (2009).
13. S. Yu, G. X. Piao, D. R. Mason, S. In, and N. Park, "Spatiospectral separation of exceptional points in PT-symmetric optical potentials," Phys. Rev. A **86,** 031802(1–5) (2012).

#177796 - $15.00 USD Received 12 Oct 2012; revised 14 Nov 2012; accepted 14 Nov 2012; published 7 Dec 2012

14. G. W. Hanson, "Dyadic Green's functions for an anisotropic, non-local model of biased graphene," IEEE Trans. Antennas Propagat. **56,** 747–757 (2008).
15. D. N. Christodoulides, and R. I. Joseph, "Discrete self-focusing in nonlinear arrays of coupled waveguides," Opt. Lett. **13,** 794–796 (1988).
16. T. Pertsch, T. Zentgraf, U. Peschel, A. Brauer, and F. Lederer, "Anomalous refraction and diffraction in discrete optical systems," Phys. Rev. Lett. **88,** 093901(1–4) (2002).

1. Introduction

Graphene is a single layer of carbon atoms packed in a honeycomb lattice which has been attracting increasing interest from the scientific community since 2010, when the Nobel Prize in Physics was assigned to Novoselov and Geim for their groundbreaking experimental results [1].

Graphene is a special material which is characterized by exceptional properties. In particular mobility of charge carriers is extremely high, thus it is expected that graphene can have an important role for future evolution of high-speed electronics, likely by improving performance of conventional silicon devices rather than by replacing them [2].

The optical properties of graphene display intriguing features over a very wide bandwidth that covers the mid-infrared and the visible spectrum. Indeed, infrared plasmonic devices based on graphene have already been proposed [3] whereas a plethora of applications at optical frequencies, ranging from photovoltaics and light-emitting devices [4] to the realization of novel components for communication systems [2, 5–9] have been reported, in spite of the small absorption which is typical of graphene layers under normal optical excitation.

In this context, deposition of graphene layers onto/into silicon waveguides which permit interaction length to be increased appears to be a promising method to realize compact broadband optical modulators [2, 5–7]. These structures exploit a simple operation principle: graphene behaves as a loss element controlled by an electric voltage, which properly tunes the electric Fermi level near the Dirac point of the conical dispersion relation [10]. In this way, graphene conductivity can be switched from 0 to an universal frequency-independent value.

In this work we present numerical results which demonstrate the huge potential of graphene as a mean to control coupling between optical waveguides. The possibility of tuning losses in each waveguide by acting on a thin loss element permits symmetry of the system of coupled waveguides to be broken without introducing a strong perturbation of the single waveguide. Remarkably we demonstrate that tunable losses induced by graphene and a careful design of ridge waveguides allows to probe passive PT-symmetry breaking in directional couplers [11–13]. Moreover we prove that the exceptional point of the proposed structure can be dynamically reached by varying the applied voltage. We will thus explore this property to mould energy exchange between waveguides and to finely tune discrete diffraction in waveguide arrays.

2. Optimal control of losses in an optical waveguide

We considered the behavior of silicon waveguides on a silica substrate in a wavelength range between 1350 and 1600 nm. The structure has been inspired by the modulator proposed in [2]. In particular, a layer of silicon with thickness equal to 50 nm is deposited onto the substrate. The 400-nm-wide ridge waveguide is composed of a lower and a higher layer made of silicon (both with thickness 200 nm) which sandwich a central region including three alternating layers of alumina (thickness 7 nm) and two absorption layers composed of three graphene monolayers with thickness 0.34 nm. Graphene can be electrically controlled in order to tune doping (and then conductivity), as suggested in [2] and [6]. The dielectric constants of silicon, silica and alumina were taken equal to 12.1, 2.1 and 3. Figure 1(a) displays a schematic view of the structure.

The behavior of graphene in the optical regime has been numerically modeled by following

#177796 - $15.00 USD Received 12 Oct 2012; revised 14 Nov 2012; accepted 14 Nov 2012; published 7 Dec 2012

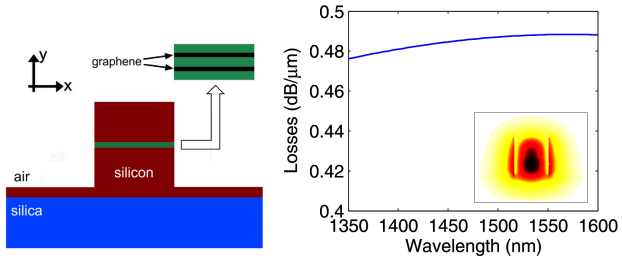

(a) (b)

Fig. 1. (a) Schematic view of the waveguide structure, with a detail of the central region with graphene layers. (b) Losses of the single waveguide (in dB/μm) when graphene is in OFF state (null voltage), and x-component of the electric field of the TE-like mode (inset).

the approach suggested in [3]. Indeed, we assigned to each graphene monolayer with thickness Δ a volume conductivity equal to $\sigma_{g,v} = \sigma_{2D}/\Delta$, where σ_{2D} is the conductivity of the 2D sheet. It was demonstrated that, as a first approximation, few-layer graphene is characterized by the same band structure (and then by the same excellent electronic properties) of the monolayer, and plus conductivity of N-layer graphene ($N = 3$ in our design) can be evaluated as N times conductivity of the single layer if N is small enough [5].

Analytical studies and experimental results (see [10, 14]) which provide the 2D conductivity from microwaves to the optical regime as a function of the driving voltage have been reported in the literature. All these works demonstrate that the optical conductivity of graphene is dominated by the interband component, which can be tuned by acting on the control voltage. In particular, the real part of graphene conductivity is close to zero below a well defined threshold frequency corresponding to the onset of interband transitions, whereas over this abrupt threshold conductivity recovers the universal value $\sigma_{2D} = \pi e^2/2h$ [10]. The threshold frequency f_{th} is located around $hf_{th} = 2E_F$, where h is Planck's constant and E_F is the Fermi level, which can be moved by acting on the applied voltage. This threshold shifts to larger frequencies with increasing voltage, and few volts are sufficient to move it in the near-infrared.

We performed a modal analysis of the waveguide in Fig. 1(a) by resorting to finite-element simulations. We focused the attention on the TE-like mode which is depicted in the inset of Fig. 1(b), since the electric field is tangential with respect to graphene layers. In the same figure we report absorption of the TE-like mode when graphene layers are in OFF state (null voltage). Of course, when graphene is in ON state (a control voltage is applied) losses are close to zero. First, it is important to note that the real part of the effective index of the mode (not shown here) is barely affected by state of the graphene layers. Then, we emphasize that when graphene is in OFF state losses are quite large (0.48 dB/μm, which corresponds to 1100 cm^{-1}) and almost constant over the entire bandwidth: indeed, a 6-dB modulation contrast between ON and OFF states can be achieved with a 12.5 μm-long waveguide. In the next paragraphs we will study properties of coupled waveguides wherein the described structure is the basic building block.

3. Coupled-mode theory

Full-wave simulations of photonic devices including graphene layers are characterized by huge computational burden. This effect is obviously emphasized when structures composed of multiple waveguides must be analyzed, therefore conventional coupled-mode theory (CMT) [15, 16] has been reformulated to study our structure. Using full wave simulations, we first numerically proved that neither profile of TE-like modes nor the propagation constant β of each isolated

#177796 - $15.00 USD Received 12 Oct 2012; revised 14 Nov 2012; accepted 14 Nov 2012; published 7 Dec 2012

waveguide are affected by the status of graphene layers, whereas switching between ON and OFF states has the effect of turning off and on losses in the single waveguide, which are modeled by the attenuation constant α. Notice that modal evolution reads as $\exp(i\beta z)\exp(-\alpha z)$.

Under these conditions it is possible to verify that the system of governing equations for $A_{1,2}$, which are the modal field amplitudes in the first and second waveguide of a directional coupler composed of two identical graphene-based waveguides, can be approximated as

$$\frac{d}{dz}\begin{bmatrix} A_1 \\ A_2 \end{bmatrix} = i\begin{bmatrix} \beta + i\alpha_1 & C \\ C^* & \beta + i\alpha_2 \end{bmatrix}\begin{bmatrix} A_1 \\ A_2 \end{bmatrix}, \tag{1}$$

where $\alpha_{1,2}$ can be tuned between 0 (ON state) and α_{max} (OFF state) by controlling the voltage applied to the graphene layers, and C is a complex coupling coefficient [12].

When $\alpha_1 = 0$ and $\alpha_2 = \alpha$ the eigenvalues read as $\lambda_{1,2} = \beta + i(\alpha/2) \pm \sqrt{|C|^2 - (\alpha/2)^2}$, with the so-called exceptional point (EP) for the onset of PT-symmetry breaking which is located at the critical loss $\alpha_c = 2C$. When $\alpha < \alpha_c$ the two supermodes have different propagation constants and the same attenuation constant $\alpha/2$. Beyond the critical loss supermodes coalesce, indeed they are characterized by equal propagation constant β and different losses. In particular, one supermode experiences increasing losses with increasing α, whereas the other one is characterized by the opposite trend [11, 12]. When α is much larger than C, one supermode is characterized by losses which are close to those of a single lossy waveguide, whereas the other one tends to be loss-free (see next section).

4. Control of coupling between optical waveguides

We examined the behavior of the directional coupler which is obtained by placing two identical graphene-based waveguides close to each other, separated by a 300-nm gap (see Fig. 2 on the left). We performed a modal analysis at 1530 nm focusing the attention on the supermodes which originate from interaction between TE-like modes of the single waveguides, and we varied the state of the graphene layers. Numerical results in Fig. 2 illustrate in a qualitative way how the behavior of the structure can be controlled by exploiting properties of graphene. In particular, when graphene layers in both the waveguides are in the same state symmetry of the structure is preserved, and the two modes (not shown here) are even and odd. Viceversa, Fig. 2 shows that when symmetry is broken by switching to the ON-OFF state the effect of losses on the modal properties is huge, and a trend toward decoupling between the waveguides is visible.

The dispersive properties of the two modes have been characterized through full-wave and CMT simulations, and these quantitative results confirm the intuitive analysis we have reported above. Indeed, in Fig. 3(a) losses of the two supermodes are depicted when graphene layers are in the ON-OFF state. In this case symmetry is broken, as a consequence one mode is characterized by absorption which is close to zero, whereas losses of the other one are large, very close to those of a single lossy waveguide. It is worth noting that this effect tends to blur with increasing wavelength due to the dependence of coupling coefficient on frequency (C gets larger with increasing wavelength). A thorough treatment on phenomena arising from the wavelength dependence of the PT-symmetry condition is reported in [13]. The noticeable agreement between

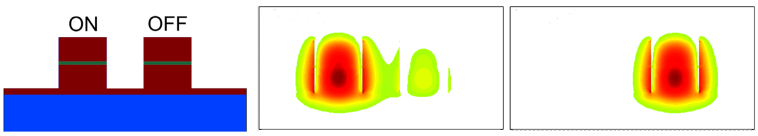

Fig. 2. Schematic view of the 300-nm-gap coupler (left), with the electric field of the low- (center) and high-loss mode (right) at 1530 nm. Graphene layers are in ON-OFF states.

#177796 - $15.00 USD Received 12 Oct 2012; revised 14 Nov 2012; accepted 14 Nov 2012; published 7 Dec 2012

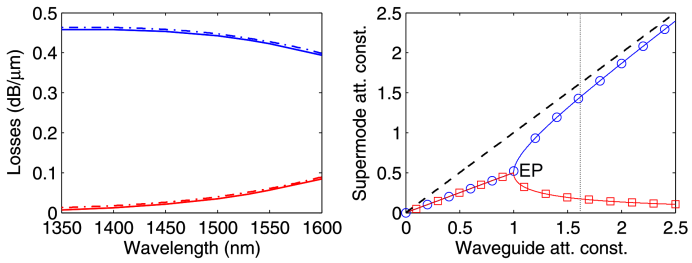

(a) (b)

Fig. 3. (a) Losses of low- (red line) and high-loss mode (blue line) from mode solver (solid line) and CMT (dashed-dotted line). (b) Normalized attenuation constant of low- (red line with squares) and high-loss mode (blue line with circles) vs. normalized attenuation constant of the single waveguide at $\lambda = 1530$ nm. The vertical thin line indicates $\alpha = \alpha_{max}$.

simulations performed by using a full-wave mode solver and results evaluated by using CMT (in the latter case the imaginary part of $\lambda_{1,2}$ is reported) allows to confirm the accuracy of CMT.

These phenomena stem from breaking of passive PT-symmetry in complex potentials. Indeed, in Fig. 3(b) we plot the attenuation constants of the two supermodes, evaluated by using CMT, as a function of the attenuation constant of the single waveguide α. Data are normalized with respect to twice the coupling coefficient, so that we have the exceptional point when the abscissa is equal to 1. The vertical dotted line indicates α_{max}, i.e. the value of α when our structure is in OFF state, and it is straightforward to see that we can work beyond the exceptional point, in agreement with the results in Fig. 3(a). It is worth to emphasize that graphene-based waveguides exhibit superior properties with respect to waveguides wherein losses are introduced by depositing metal layers [12]. Losses induced by sandwiching graphene layers inside silicon waveguides can be orders of magnitude larger (thousands of cm^{-1} with respect to tens of cm^{-1}), therefore it is possible to probe the exceptional point even in structures characterized by strong coupling. Last, but not least, it is important to note that graphene is electrically tunable, therefore losses in each single waveguide can be varied between 0 (ON state) and a maximum value α_{max} determined only by geometry (OFF state).

We envisage that switching of the state of one waveguide can be exploited to finely tune coupling between waveguides. In order to verify the effectiveness of this approach we applied CMT to our reference structure at the wavelength of 1530 nm, and we show the results in Fig. 4. When the coupler is in the ON-ON state losses are zero, and the predicted beat length

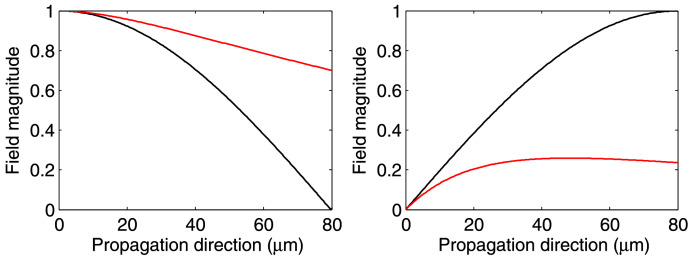

(a) (b)

Fig. 4. Field amplitude in (a) first and (b) second waveguide of the coupler. Graphene layers are in ON-ON (black line), and ON-OFF (red line) states.

#177796 - $15.00 USD Received 12 Oct 2012; revised 14 Nov 2012; accepted 14 Nov 2012; published 7 Dec 2012

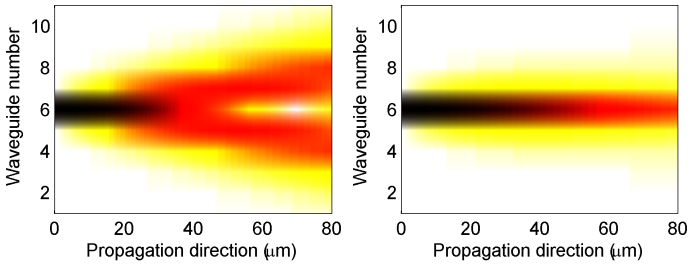

(a) (b)

Fig. 5. Discrete diffraction along the array. (a) All the graphene layers are in ON state. (b) Only graphene layers inside the central waveguide are in ON state.

$L_B = \pi/(\beta_{even} - \beta_{odd})$ is around 80 μm. Viceversa, when graphene layers are ON and OFF in the input and output channel the two waveguides tend to decouple and field intensity in the first waveguide is larger than in the second one. It is possible to justify this behavior by recalling that when we inject light into the waveguide in ON state the low-loss supermode is mainly excited.

These results have been validated by comparison with simulations of the 80-μm long coupler performed by using the commercial software CST Microwave Studio, which allows to solve Maxwell's equations in the time domain through the finite-integration technique. Indeed, the ratio between output and injected power evaluated by using CMT is -3 and -12 dB if coupler is in ON-OFF state and we consider as output port waveguides 1 and 2. CST simulations exhibit a good agreement, in fact the corresponding calculated values are about -5 and -13 dB.

5. Control of discrete diffraction in optical waveguide arrays

The unique properties we have described in the previous paragraph open the way to novel possibilities for controlling discrete diffraction in waveguide arrays [15, 16]. Let us take for example an array composed of 11 identical waveguides, with the same geometrical and optical parameters we have used throughout the work, and the same spacing (300 nm) we have considered in the case of the coupler. The structure is simulated by using CMT in order to reduce the computational burden. The input excitation covers only the central waveguide, and the propagation length is taken equal to the beat length of the coupler (80 μm). Moreover, we assume that state of graphene layers in each waveguide can be controlled independently from each other.

In Fig. 5(a) we show the field inside the structure when all the graphene layers are in ON state: the typical pattern of discrete diffraction is clearly visible, with two pronounced outermost wings [15, 16]. In Fig. 5(b) all the waveguides except the central one are switched to the OFF state, and two phenomena can be clearly noticed. First, beam broadening is reduced with respect to the previous case, and most of the optical energy remains concentrated into the central waveguide. Then, losses are smaller with respect to the case of a single lossy waveguide.

6. Conclusion

We have presented properties of graphene-based coupled waveguides. In particular, we have shown that tuning the state of graphene layers in each single waveguide allows energy exchange between the two channels of a coupler and discrete diffraction in arrays to be controlled.

Acknowledgments

AL and CDA acknowledge financial support from Cariplo Foundation under grant no. 2010-0595, and from US Army under grant no. W911NF-12-1-0202.

#177796 - $15.00 USD Received 12 Oct 2012; revised 14 Nov 2012; accepted 14 Nov 2012; published 7 Dec 2012